Applied Acoustics 95 (2015) 50–56

Contents lists available at ScienceDirect

Applied Acoustics

journal homepage: www.elsevier.com/locate/apacoust

Reducing interior noise in a cylinder using micro-perforated panels

Cheng Yang, Li Cheng *, Zhongyu Hu

Department of Mechanical Engineering, The Hong Kong Polytechnic University, Hung Hom, Kowloon, Hong Kong Special Administrative Region

ARTICLE INFO

Article history:
Received 14 November 2014
Received in revised form 9 February 2015
Accepted 10 February 2015
Available online 17 March 2015

Keywords:
Micro-perforated panel
Cylindrical enclosure
Acoustic coupling

ABSTRACT

Sound absorption inside a cylindrical enclosure using micro-perforated panels (MPP) is investigated. Attention is focused on analyzing the effect of backing cavities on the sound absorption capabilities of various MPP configurations both numerically and experimentally. A model is used to analyze the acoustic coupling between the cylindrical acoustic domain enclosed by the MPP and the annular cylindrical acoustic domain forming the air space behind it. It was shown that the sound field in the backing cavity of the MPP plays an important role in determining the energy dissipation efficiency of the MPP construction, and thereby affects the degree of attenuation of the standing waves inside the enclosure. Conventional MPP construction with a backing air layer was shown to only provide limited noise reduction, but fail at certain frequencies associated with the acoustic resonances of the cylindrical acoustic field. The problem can be tackled by adding proper partitions in the baking cavity, as a result of the alteration of the acoustic coupling across the MPP panels.

1. Introduction

The pioneer work on micro-perforated panel (MPP) can be traced back to nearly forty years ago. By expanding the short tube theory, Maa's work [1] allows the theoretical prediction of the acoustic impedance of a MPP. To achieve effective sound absorption, an air gap is usually placed between the MPP and a backing rigid wall so as to produce the Helmholtz resonance effect. Without considering the panel vibration, the acoustic impedance of the MPP is independent of the material properties. Hence, it can be fabricated by waterproof, heatproof or flameproof materials, making it a good alternative to conventional fibrous and porous materials in numerous acoustic applications [2–15].

Generally speaking, two major parameters are usually used to quantify the acoustic property of a MPP construction: the sound absorption coefficient and the normal acoustic impedance over its surface. With MPP construction placed on a wall, both parameters are widely used by treating the MPP as equivalent acoustic boundaries. Those two quantities, however, may not truthfully represent the *in-situ* working condition of the MPP when it is integrated into a compact acoustic system. Recent work [16] showed that two MPP constructions, one with a partitioned backing air space and the other one without, give the same sound absorption curves in the impedance tube test, but exhibit totally different sound absorption behaviors when placed on the wall of a rectangular enclosure. The work indicated that the acoustic behavior of the MPP could be strongly influenced by the acoustic media coupled across the MPP, which is drastically different from the free field configuration. Indeed, a MPP dissipates acoustic energy through Helmholtz resonance absorption inside the holes, as a result of the pressure difference between the two sides of the MPP. In this sense, how the sound pressure field behind MPP behaves will, in principle, affect the dissipation capability of the MPP. More recently, Toyoda et al. [17] and Yu et al. [18] noticed that even the conventionally used backing air cavity behind the MPP is not always necessary, provided a pressure difference between the two sides of MPP is formed. Despite these observations and hypotheses, thorough analyses which allow clear understanding of the underlying physics are still lacking. This motivates the present work to take a closer look at the MPP construction by undertaking a systematic analysis of the working mechanism of the MPP in the presence of the acoustic coupling across its surface.

As a benchmark problem, the interior sound field inside a cylindrical enclosure with an inner MPP liner is investigated. The MPP liner consists of a folded MPP with various backing configurations. Particular attention is paid to studying different configurations of the backing air space of the MPP liner. Note that the cylindrical enclosure is also of considerable importance in many engineering applications such as aircraft fuselage, ventilation duct and Magnetic Resonance Image (MRI) scanner. It is also relevant to note that in a previous work, Li and Mechefske [19] examined the possibilities of using MPP liner to reduce the noise level in the MRI scanner bore. The backing air space of the MPP is left

* Corresponding author. Tel.: +852 2766 6769.
E-mail address: li.cheng@polyu.edu.hk (L. Cheng).

http://dx.doi.org/10.1016/j.apacoust.2015.02.003
0003-682X/

empty without any particular treatment. Measurements showed that although MPP could reduce the interior noise to some extent, it is not so effective in some cases. A later investigation by Fraser [20] reported that the noise reduction is not sufficient for significant differences in perceptions by volunteers tested in MRI experiment. The present paper will provide an answer to these observed phenomena. As will be demonstrated later, the noise suppression capability of the MPP can be improved with proper treatment to the backing air space. The general understanding of the underlying physics could also assist in improving the noise control performance of MPPs in other applications.

2. Numerical analyses

2.1. Model development

Under a cylindrical coordinate system, an annular cylinder of outer radius $r1$, inner radius $r2$, and length L is shown in Fig. 1. Assuming an acoustically rigid outer wall, the inner cylindrical wall represents a MPP boundary with:

$$v_1 = \frac{p_1 - p_2}{Z_{MPP}} \tag{1}$$

$$v_1 = -v_2 \tag{2}$$

where p_i is the sound pressure on the MPP surface, v_i is the averaged normal air particle velocity over the MPP surface (positive outward), and Z_{MPP} is the acoustic impedance of the MPP given by Maa [1]. Subscript 1 and 2 denote the two acoustic domains, respectively, *i.e.* the one between the two cylindrical walls; and the other enclosed by the inner cylindrical MPP wall. The two terminations of the acoustic domains are assumed to be acoustically rigid.

With a point source inside acoustic domain 2, the air motion inside the MPP pores becomes a secondary source, radiating sound into domains 1 and 2 simultaneously. In harmonic regime, the sound pressure field in domain 2 can be described by the Kirchhoff–Helmholtz integral equation [21] as

$$p_2 = -j\rho\omega \int_{S_a} G_2 v_2 dS_a + \int_{V_s} G_2 Q dV_s \tag{3}$$

where G_2 is the Green's function, Q has the expression of $Q = j\rho\omega q\delta(r - r_s)\delta(x - l_s)$ with ρ, ω, q, $\delta(-)$, r_s, l_s being respectively, the air density, angular frequency, volume velocity of the point source, the Dirac delta function, the radial and longitudinal distances of the point source. r and x are the radial and longitudinal distances of the observing point. S_a is the surface occupied by MPP and V_s is the volume of the point source.

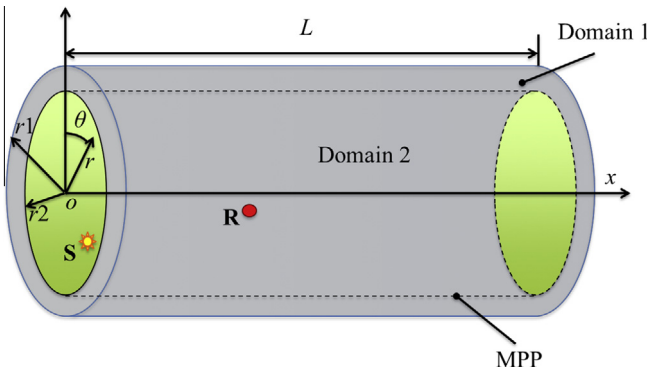

Fig. 1. Diagram for the MPP lined on the inner wall of a cylindrical acoustic domain, a uniform air space of depth $r1 - r2$ is left behind the MPP.

Table 1
Parameters of the cylinder and MPP in simulation.

Cylinder	MPP	
$r1$ = 230 mm	Diameter of the hole	0.35 mm
$r2$ = 200 mm	Panel thickness	0.35 mm
l = 400 mm	Perforation ratio	1%

Similarly, the sound field in domain 1 is also determined by the velocity on MPP surface:

$$p_1 = -j\rho\omega \int_{S_a} G_1 v_1 dS_a \tag{4}$$

The rigid-walled modes of the two domains can be expressed analytically [22–24]. For domain 1 (annular cylindrical cavity), the Mth rigid-walled mode ϕ_M is expressed as:

$$\phi_M(r,x) = \begin{Bmatrix} \cos(m\theta) \\ \sin(m\theta) \end{Bmatrix} * \left(J_m(k_{mn}r) - \frac{J'_m(k_{mn}r2)}{Y'_m(k_{mn}r2)} Y_m(k_{mn}r) \right) * \cos\left(\frac{p\pi x}{L}\right) \tag{5}$$

where k_{mn} is the zero of the cross-product of Bessel function and θ is the azimuthal angle.

$$J'_m(k_{mn}r2)Y'_m(k_{mn}r1) - J'_m(k_{mn}r1)Y'_m(k_{mn}r2) = 0 \tag{6}$$

In Eqs. (5) and (6), J_m and Y_m are the Bessel functions of the first and second kind of order m, respectively; the prime indicates the first derivative; L is the length of the cylinder; m, n, p are the circumferential, radial longitudinal order, respectively.

For domain 2 (cylindrical cavity), the Nth rigid-walled mode ψ_N writes

$$\psi_N = \begin{Bmatrix} \cos(m\theta) \\ sin(m\theta) \end{Bmatrix} * J_m(k_{mn}r) * \cos\left(\frac{p\pi x}{L}\right) \tag{7}$$

where k_{mn} satisfies the following equation

$$J'_m(k_{mn}r2) = 0 \tag{8}$$

The Green's functions G_1 and G_2, which describe the response at (r,x) due to point source excitation at (r',x'), can be constructed by the corresponding rigid-walled modes in each domain as

$$G_1(r,r',x,x') = \sum_M \frac{\phi_M(r,x)\phi_M(r',x')}{\Lambda_{1M}\left(k_{1M}^2 - k^2\right)} \tag{9}$$

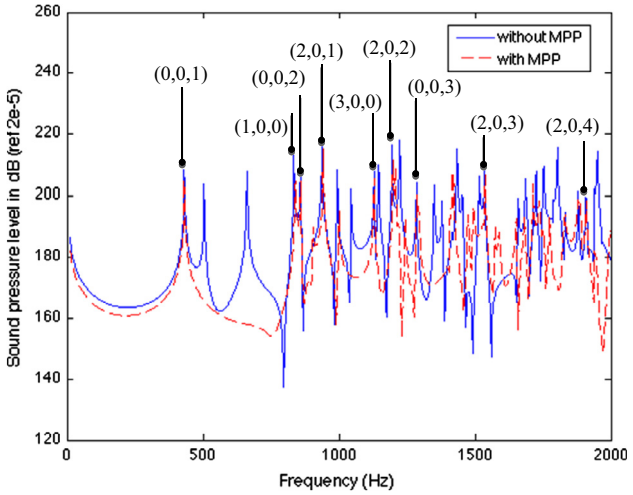

Fig. 2. Simulated interior sound pressure level.